Data-Driven Inverse Control of Pneumatic Soft Robotic Actuators with On-Off Valves: Simulated Performance

1st Taylor R. Young
School of Engineering
The University of Newcastle
Callaghan, Australia
taylor.young@newcastle.edu.au

2nd Yuen K. Yong
School of Engineering
The University of Newcastle
Callaghan, Australia
yuenkuan.yong@newcastle.edu.au

3rd Andrew J. Fleming
School of Engineering
The University of Newcastle
Callaghan, Australia
andrew.fleming@newcastle.edu.au

2025 IEEE International Conference on Mechatronics (ICM) | 979-8-3315-3389-2/25/$31.00 ©2025 IEEE | DOI: 10.1109/ICM62621.2025.10934841

***Abstract*—This article describes a data-driven control method for fast and accurate pressure regulation of pneumatic soft robotic actuators with on-off valves. Due to the non-linearity and binary control input, linear controllers are not ideal for pressure regulation as they must be tuned conservatively, which results in a slow transient response. Alternatively, non-linear methods can provide a faster response time but are complicated by the need for an accurate model. This article proposes an inverse control approach, where the control action is parameterized by the valve on-time, and the system output is the cumulative change in pressure after the control action is complete and all system transients have decayed. This approach eliminates the need for a dynamic model and results in a small space of input-output combinations that can be measured from a calibration experiment. The result is a non-linear inverse controller that does not require a dynamic model.**

The proposed method is compared in simulation to a hysteresis controller with three different valve orifice diameters. Significant improvements to the pressure regulation and valve lifetime are observed. This method is expected to find applications in soft robotics where fast step changes and dynamic trajectories are required.

***Index Terms*—Soft Robotics, identification and control methods, time-based control, non-linear control**

I. Introduction

Fluidic soft robots are typically driven by a system of pumps and valves [1], [2], [3]. Their applications include minimally invasive surgery [4], rehabilitation [5], [6] and elderly assistance [7]. Compared to rigid robots, soft robots provide a desirable combination of high compliance, low mass, and user safety. Soft robots are typically driven by a pneumatic source with on-off valves for pressurization and discharge.

Various configurations of solenoid valves have been described in the soft robotics literature [8], [9], [10]. Valves with three ports and two positions, known as 3/2 valves, permit either charging or discharging the actuator. These systems have no stable operating point and are not well suited to applications that require arbitrary pressure references. Alternatively, two 'on-off' or 2-port 2-position valves can be used [9], [10]. This configuration allows for a stable operating point where air is neither entering nor exiting the actuator.

In this article, two on-off valves will be considered as these offer reduced energy consumption, reduced pressure ripple and improved lifetime due to a reduced number of switching events, particularly for constant pressure set-points [11].

As outlined in [1], [12], [13], [14], [15] conventional model-free methods of control are difficult due to their significant degrees of freedom and highly nonlinear dynamics [16], [17]. As such these controllers always trade off the overshoot/undershoot behavior with the rise and settling time of the system response. The hyper-elasticity, pneumatic compressibility, nonlinearity of valve flow and actuation time complexities result in a complex nonlinear system [18], [19], [20].

Like model-free controllers, dynamic model-based controllers are also difficult due to the highly non-linear model structures. Whilst many efforts to design model-based controllers have been made, existing model-based static controllers require manual tuning of the model parameters, with high sample times for the control strategies and are mostly suited to reference signals with low-frequency components. Common static model-based controllers are developed on piecewise constant curvature assumptions or an incompressible Neo-Hookean model [1]. Adaptive controllers with inverse feed-forward paths have also been utilized in [8].

The binary nature of the valves constrains the control problem associated with the two-valve system. The control command has three discrete states. Model-based approaches are not well suited to this application for the following reasons. First, pneumatic systems are non-linear and difficult to include in prediction algorithms. Second, soft actuators are highly non-linear pneumatic loads, with large uncertainties between actuators. Third, the solenoid valves exhibit significant time delay and minimum on-time, dependent on the operating pressure. These difficulties significantly impede the application of model-based inverse control methods.

In this article a hysteresis controller was chosen as the comparison controller due to their simple implementation, wide spread comparative use throughout soft robotic literature, and their minimal switching behavior when tuned with

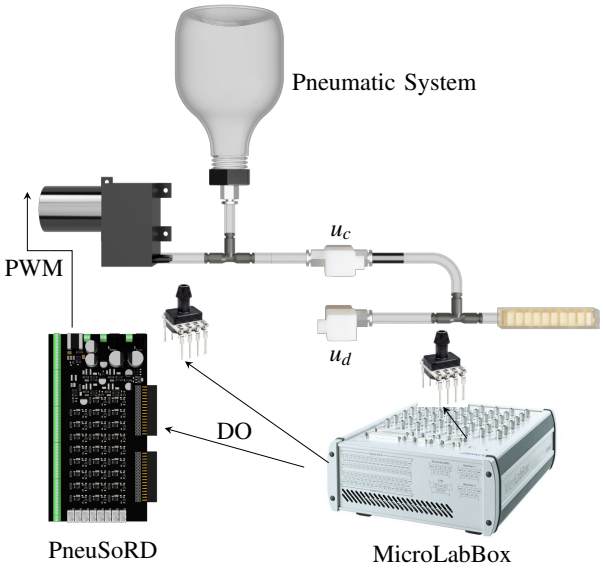

Fig. 1: Target system overview. The setup includes a diaphragm pump (KYK50BPM), a 2 L air receiver, two on-off solenoid valves (VDW22LA, SMC), two pressure sensors (SSCDANV015PGAA5, Honeywell) and 6 mm tubing. The system is controlled via a dSPACE MicroLabBox

an appropriate window size. Other control methods typically exhibit an order of magnitude or more switches to achieve control performance.

A. Contributions of this work

This article describes a practical method for improving the performance of pressure control systems by using an initialization step to identify samples of an inverse model. Since the controller command is binary, the controller response can be parameterized by the required on-time of the solenoid valves. The space of possible control commands is small enough to experimentally generate a lookup table that relates the valve on-time and initial pressure to the resulting pressure change. By inverting this table and utilizing an interpolation approach, a data-driven inverse time controller is implemented.

The proposed method is compared in simulation to a hysteresis controller with three orifice diameters. Initial results show significant improvements to the pressure regulation and valve lifetime. Applications are expected to include soft grippers, catheter devices, robotic fingers, and robotic hands.

The comparison controller and limitations are defined in Section II, followed by the inverse control concept in Section III. The simulation model and control algorithm are described in Sections IV and V, followed by simulation results in Section VI.

II. Hysteresis Control and Limitations

The soft robotic control system in Fig. 1 includes a single valve for charging the actuator, and a single valve for discharging. Such systems are typically controlled by a hysteresis controller with three discrete states. In the charging state, the charging valve is open while the discharge valve is closed, i.e. $u_c = 1$ and $u_d = 0$. In the resting state, both valves are closed, i.e. $u_c = 0$ and $u_d = 0$. In the discharge state, the discharge valve is open and the charging valve is closed, i.e. $u_c = 0$ and $u_d = 1$.

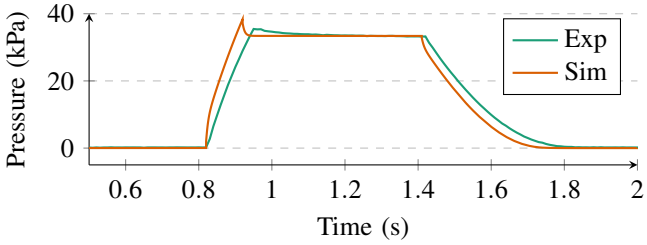

Fig. 2: Experimental vs Simulated approximation of a soft robotic actuator modeled as a piston with initial dead volume connected to a mass spring damper. 0.1 s Rise time for inflation using a 0.9 mm valve. When the inflation valve is switched off, the actuator elasticity relaxes, causing the pressure to drop the the static pressure point.

For hysteresis control when the pressure error is greater than h_{on}, the charging state is activated. As the error decreases, the valve remains on until the pressure error is less than h_{off}. Similar behavior occurs when the pressure error is negative, therefore, four parameters define the behavior. Typically, the h_{off} parameter is set to 0. The hysteresis control command is determined by a series of inequalities for each valve:

$$\text{Charge Valve} \begin{cases} \text{Switch on,} & P_{ref} - P_A > h \quad (1a) \\ \text{Switch off,} & P_{ref} - P_A = 0 \quad (1b) \end{cases}$$

$$\text{Discharge Valve} \begin{cases} \text{Switch on,} & P_{ref} - P_A < -h \quad (2a) \\ \text{Switch off,} & P_{ref} - P_A = 0 \quad (2b) \end{cases}$$

where: h represents the hysteresis.

One limitation of model-free controllers is the steady-state error caused by the hyper-elastic settling time of the actuator. As shown in Fig. 2 when a soft robotic actuator is inflated, the pressure inside the actuator increases at some rate dependent on the actuator, the upstream pressure and the orifice diameter of the valve. This response is relatively fast compared to the actuator settling time. When the inflation valve is turned off the actuator's elastic response settles, causing the final pressure in the actuator to drop below the pressure achieved at the instant the valve was switched. This introduces steady-state control error. The elastic response relaxation amount is worse for steps with higher flow rates, and hence, larger valve diameters. For a controller to overcome these issues, it must take into account both the minimum opening time of a pneumatic valve and the static response of the actuator.

III. Inverse Control Overview

The inverse controller aims to estimate the required time a valve must be actuated to reduce the pressure error to zero.

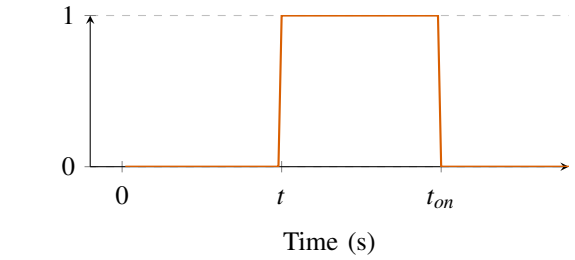

(a) A step input signal to the plant P(s) with variable pulse width t_{on}.

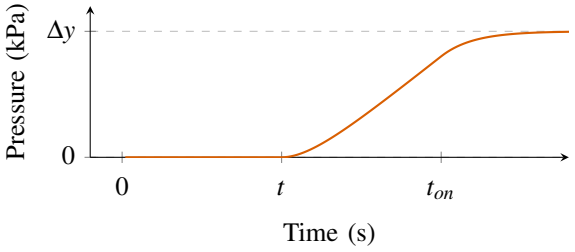

(b) Output response of the plant in Eq. 4

Fig. 3: Output response of the plant in Eq. 4 which is driven by a step input signal with variable pulse width t_{on}.

A. Inverse Control Derivation

Focusing solely on the inflation scenario, the control input is reduced to a binary choice: on or off. This discrete input, combined with the plant's complex dynamics, creates challenges in controlling the system effectively.

1) Single input problem: Consider a single input-output system $P(s)$ with input $U(s)$, the output $Y(s)$ is

$$Y(s) = P(s)U(s). \tag{3}$$

For the sake of example, consider the following plant which approximates a soft robotic actuator with integral action and relaxation,

$$P(s) = \frac{1}{s} - \frac{1}{s+10}. \tag{4}$$

Consider the control action in Fig. 3a which consists of a pulse with duration t_{on}. The Laplace transform is

$$U(s) = \frac{1}{s} - \frac{e^{-t_{on}s}}{s}. \tag{5}$$

The system output Fig. 3b responds to $U(s)$ with a change Δy. For system Eq. 4, the response to an input pulse of duration t_{on} is

$$Y(s) = \left(\frac{1}{s} - \frac{1}{s+10}\right) \times \left(\frac{1}{s} - \frac{e^{-t_{on}s}}{s}\right) \tag{6}$$

By applying the Final Value Theorem and a Taylor Series approximation, the change in the plant output after all transients have decayed is

$$\Delta y = t_{on}, \tag{7}$$

that is, the change in the plant output after the control cycle is complete and all transients have decayed can be directly related to the on-time duration. Equivalently, the on-time of the actuator can be determined from only the required output change (or pressure error in soft robotic applications).

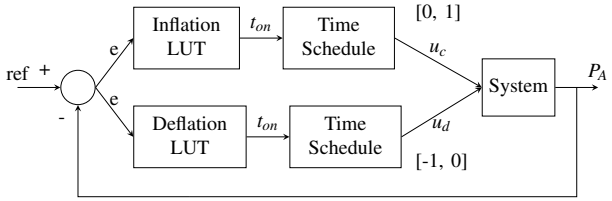

Fig. 4: Control loop diagram showing the inverse controller loop

To generalize the above result, consider the arbitrary system

$$\Delta y = f(t_{on}) \tag{8}$$

where f may be dependent on other parameters such as the current operating pressure or source pressure. The valve on-time which achieves an output change Δy is

$$t_{on} = f^{-1}(\Delta y) \tag{9}$$

2) Soft Robotic Applications: To adapt this method to soft robotic systems, Δy must be measured after the control action ceases and the system reaches steady state. Pneumatic systems also include a strong non-linear dependence on the initial pressure y_i before the control action is applied, which can be expressed explicitly

$$t_{on} = P^{-1}(\Delta y, y_i) \tag{10}$$

This method is applied to both inflation and deflation inputs individually, resulting in the controller shown in Fig. 4.

B. Lookup Table

To determine the valve on-time required to eliminate a pressure error, a lookup table is required that describes the static system behavior. This is achieved by sequentially varying the initial pressure conditions and the valve on-time, while measuring the change in output pressure. The lookup table is generated coarsely over the operating range of the actuator and results in the inflation and deflation mappings plotted in Fig. 5a and 5b.

This data is inverted from an initial pressure and time axis and remapped to a uniform grid spacing over the initial pressure and pressure error axis. This results in efficient computation of the required on-time using a simple two-dimensional lookup table with linear interpolation.

The lookup table also captures the minimum switching time of the pneumatic system, which eliminates unnecessary switching attempts when the pressure error is too small. This improves performance compared to a hysteresis controller's static hysteresis band by representing the minimum pressure error as a non-linear curve across the operating region.

The control loop uses the pressure error and current pressure to determine the required actuation time t_{on}. A trigger is then set which activates the valve for t_{on} seconds. This inverse control strategy is data-driven and completely determined

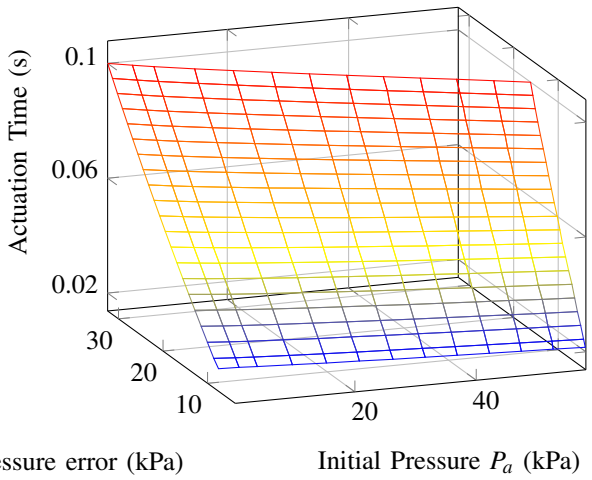

(a) The inflation lookup table for an orifice of diameter 0.9 mm

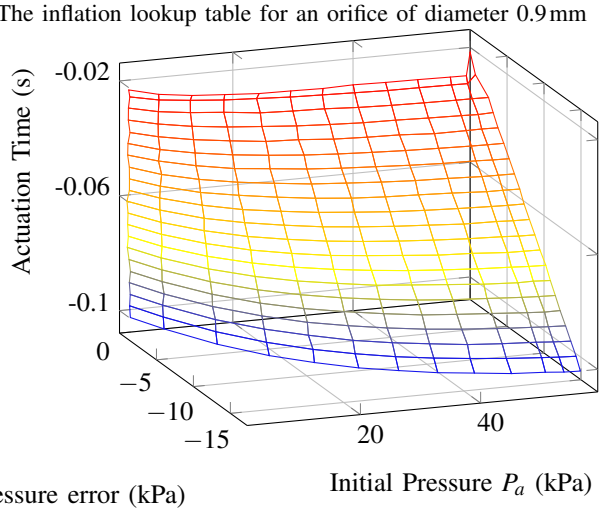

(b) The deflation lookup table for an orifice of diameter 0.9 mm

Fig. 5: The static inflation and deflation lookup tables for a simulated orifice of 0.9 mm.

by the calibration experiment; that is, there are no tuning parameters. However, the physical orifice diameter needs to be chosen appropriately to achieve a desirable trade-off between the rise-time and minimum achievable pressure change.

IV. Modeling and Simulation

A simulation model for the system in Fig. 1 was developed using Simscape Fluids and Simulink. As shown in Fig. 6, the model includes a flow-rate source, accumulator, pipes, valves, and an actuator modeled by a piston with initial dead volume connected to a mass spring damper. This piston mass spring damper system approximates the elastic relaxation that occurs and was experimentally fit to the simulated system. The simulation uses large orifice on/off valves in series with smaller orifices to represent the target system valves described in Section IV-A. The ideal controlled volumetric flow source is set to a reference pressure of 100 kPa.

A. Target System

The simulations were developed and parameterized based on an existing target system. This system in Fig. 1 includes a diaphragm pump, a 2 L air accumulator, four 2/2 on-off solenoid valves, two pressure sensors and 6 mm tubing between each of these components. The system is designed to be implemented in Simulink and dSPACE with a MicroLabBox connected to a PneuSoRD driver [11]. The actuator was constructed using a standard molding procedure [21], [22].

The target system is designed to achieve the following specifications:

- 10 % to 90 % Rise time $\leq$ 200 ms
- Accuracy $\leq$ 2 kPa

The large orifice was selected experimentally by measuring the rise time with a range of orifice diameters. An orifice with 0.9 mm diameter resulted in a 10 % to 90 % rise in 0.19 s. The small orifice was chosen to achieve a pressure change of less than 2 kPa when the initial pressure is zero, i.e. when the pressure difference across the valve is maximum. A diameter of 0.35 mm was found to result in 1.60 kPa pressure change for the minimum valve opening time. The medium orifice was chosen midway between the small and large diameters. In summary, the orifice diameters are:

- Small Valve - 0.35 mm
- Medium Valve - 0.6 mm
- Large Valve - 0.9 mm

B. Lookup Table Population

The lookup table is generated by simulating the pressure change that occurs after a valve opening cycle, for a range of valve on-times and initial pressures. The initial pressures defined as a vector $[0, 2.5, 5, 10, ..., 50, 55]$, and valve on-times linearly spaced between 0.02 s and the valve maximum on-time across 51 steps. Each valve, small, medium and large were assigned a maximum on-time of 5.0, 0.9 and 0.4 s respectively. This table is then rearranged so that the inputs are pressure error and initial pressure, and the output is valve on-time.

V. Controller Implementation

A. Inverse Controller

The inverse controller is implemented by a Simulink two-dimensional lookup table with some additional control logic. This dataset is processed in real time to output the required valve on-time. The controller runs with a local sample time trigger of 0.01 s. Around this, a reference monitors changes in the setpoint reference. When this occurs, the controller is triggered to run, searching for a time from the two-dimensional lookup table. Once a time setpoint is found, this on-time is loaded into the trigger system and applied. The reference tracking occurs asynchronously from the local sample time of the controller.

The performance of this system is compared to a hysteresis controller which has been tuned to avoid unnecessary valve activation.

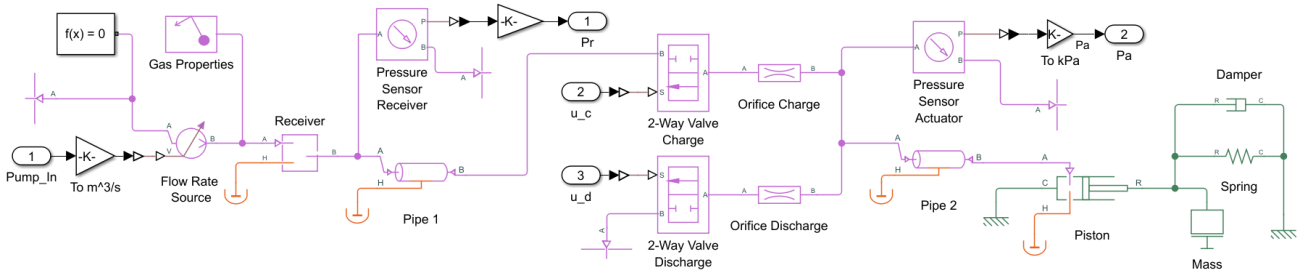

Fig. 6: Simulink model of the pneumatic system. The pneumatic components are shown in magenta and include an air compressor modeled by a controlled volumetric flow source. Transmission pipes represent the pneumatic lines. A piston with initial dead volume connected to a mass spring damper is used to model the actuator. (Model available from the first author.)

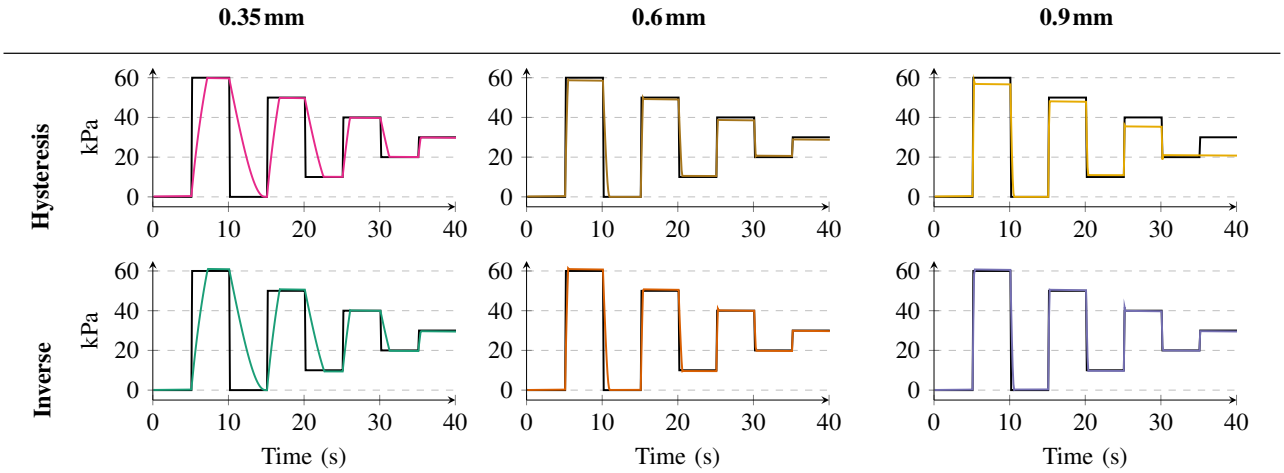

Fig. 7: Simulated comparison of the hysteresis and inverse controllers with large step changes in reference pressure over a range of conditions. The pressure reference is a decreasing amplitude square wave with a period of 10 s. Three different orifice diameters are compared. The top row is the response of the hysteresis controller, and the bottom row is the proposed controller. The columns compare different valve diameters.

TABLE I: Hysteresis values for the inflation and deflation of each orifice size.

Orifice	Inflation (kPa)	Deflation (kPa)
0.35 mm	1.38	0.62
0.6 mm	7.74	3.47
0.9 mm	14.42	6.56

B. Hysteresis Controller

The h_{on} hysteresis limits in Table I, are chosen slightly greater than the pressure resolution of the system, i.e. the minimum achievable pressure change over all operating conditions. These values were found by analyzing the step input response of each valve. The maximum pressure change that occurs in 20 ms is taken as the hysteresis limit for each valve.

VI. Results

A. Large Step Response

Fig. 7 compares the ability of each system to follow large step changes in reference pressure over a range of conditions. The response of the small valves for both controllers is limited by the flow rate through the orifice. These two responses are almost equal. For the large valve, an improvement in the RMS tracking error is observed in Table II. The inverse controller significantly improves the steady-state error compared to the hysteresis controller.

B. Small Step Response

In Fig. 8 the small step response compares the ability of each system to follow a 2 kPa pressure change over a wide range of conditions. The small valve is able to track the step changes with minimal difference in steady-state error. The response of the medium valve results in more switching, with a significant decrease in steady-state error. With large valves, the inverse controller is able to track significant more of the step changes.

C. Dynamic Response

In Fig. 9 the dynamic response compares a sinusoidal pressure reference increasing in frequency from 0.1 Hz to 1 Hz over a 100 s period. Both small valve simulations show

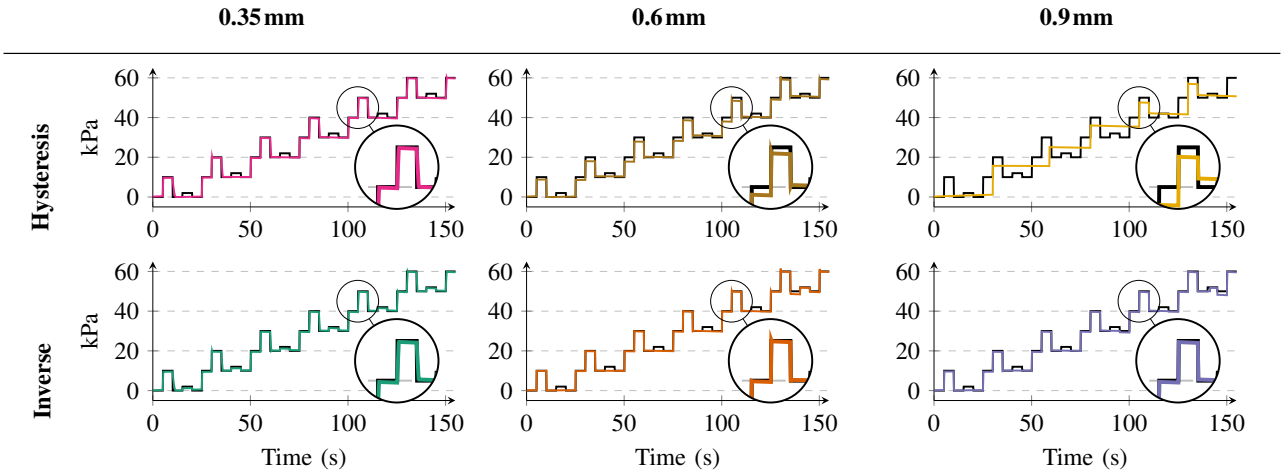

Fig. 8: Simulated comparison of the hysteresis and inverse controllers with small step changes in the reference pressure. These responses compare the ability of each system to follow a 2 kPa and 5 kPa pressure change over a wide range of conditions.

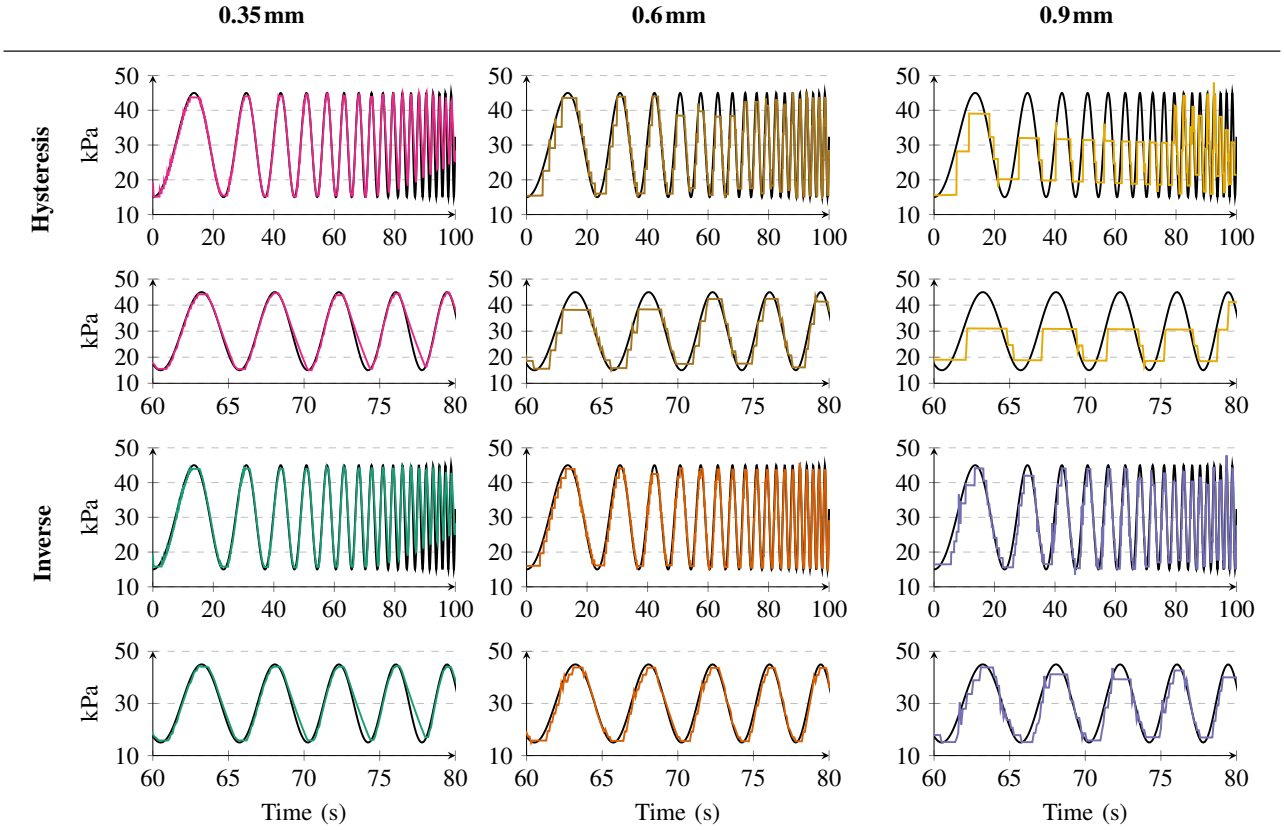

Fig. 9: Simulated comparison of the hysteresis and inverse controllers to a sinusoidal pressure reference increasing in frequency from 0.1 Hz to 1 Hz over a 100 s period. A zoomed view of the higher frequency range for each respective response is shown under each plot.

good tracking at low frequency but are eventually limited by slew-rate. In the medium and large valve simulation, the inverse controller provides a significant improvement over the hysteresis controller, albeit with more switching events. With large valves, the inverse controller significantly improves performance with good tracking across the entire frequency range.

TABLE II: The RMS tracking error and switching events from Figs. 7, 8 and 9. The inverse controller shows significant improvement for large orifice sizes.

Orifice 0.35 mm				
Test signal	***Control Method***	***RMSE***	***SS RMSE***	***Switches***
Large Step	Hysteresis	14.77	0.22	7
	Inverse	14.56	0.49	9
Small Step	Hysteresis	1.58	0.96	18
	Inverse	1.14	0.45	37
Dynamic	Hysteresis	3.17	0.70	358
	Inverse	3.45	1.07	785
Orifice 0.6 mm				
Large Step	Hysteresis	6.14	0.98	7
	Inverse	6.30	1.90	12
Small Step	Hysteresis	1.36	1.29	18
	Inverse	1.01	0.93	26
Dynamic	Hysteresis	3.37	3.41	211
	Inverse	2.04	2.12	670
Orifice 0.9 mm				
Large Step	Hysteresis	5.73	4.20	6
	Inverse	4.51	1.85	9
Small Step	Hysteresis	5.22	5.21	7
	Inverse	1.00	0.98	26
Dynamic	Hysteresis	7.18	7.16	103
	Inverse	3.34	3.32	425

D. Performance Comparison

Overall, the inverse controller significantly improves the response time and accuracy, especially for large orifice sizes. The RMS error and switching events for each simulation are summarized in Table II.

VII. Conclusion

This article describes a data-driven inverse control method for improving the speed and accuracy of pressure control systems for soft robotic actuators. Simulations are performed to compare the proposed method to an optimally tuned hysteresis controller over a range of typical operating conditions. The inverse controller significantly improves pressure regulation, while increasing the valve life-time by reducing the number of switching events. This method is suited to applications that require fast step changes and dynamic trajectories, for example, soft grippers, catheter devices, and soft robotic fingers. In these applications, the improved performance justifies the increased implementation complexity. Although the data-driven approach requires more software than a hysteresis controller, it also eliminates the need for controller tuning, and can be automatically re-calibrated after a system change.

Future work involves experimental application to a range of soft-robotic applications, and the creation of a software library that implements the calibration process and real-time inverse control. The end-goal of this work is to create an easy-to-apply pneumatic control package that provides performance at the physical limits of the valves and pneumatic system.

References

[1] P. Polygerinos, N. Correll, S. A. Morin, B. Mosadegh, C. D. Onal, K. Petersen, M. Cianchetti, M. T. Tolley, and R. F. Shepherd, "Soft robotics: Review of fluid-driven intrinsically soft devices; manufacturing, sensing, control, and applications in human-robot interaction," *Adv. Eng. Mater.*, vol. 19, no. 12, p. 1700016, 2017.

[2] B. Gorissen, D. Reynaerts, S. Konishi, K. Yoshida, J.-W. Kim, and M. De Volder, "Elastic inflatable actuators for soft robotic applications," *Adv. Mater.*, vol. 29, no. 43, 2017.

[3] M. S. Xavier, A. J. Fleming, and Y. K. Yong, "Finite element modeling of soft fluidic actuators: Overview and recent developments," *Adv. Intell. Syst.*, vol. 3, no. 2, p. 2000187, 2021.

[4] M. Runciman, A. Darzi, and G. Mylonas, "Soft robotics in minimally invasive surgery," *Soft Robot.*, vol. 6, no. 4, pp. 423–443, 2019.

[5] P. Polygerinos, S. Lyne, Z. Wang, L. Nicolini, B. Mosadegh, G. Whitesides, and C. Walsh, "Towards a soft pneumatic glove for hand rehabilitation," in *Proc. IEEE/RSJ IEEE Int. Conf. on Intelligent Robots and Systems*, 2013, pp. 1512–1517.

[6] M. Wehner, B. Quinlivan, P. M. Aubin, E. Martinez-Villalpando, M. Baumann, L. Stirling, K. Holt, R. Wood, and C. Walsh, "A lightweight soft exosuit for gait assistance," in *Proc. IEEE Int. Conf. on Robotics and Automation*. IEEE, 2013, pp. 3362–3369.

[7] Y. Ansari, M. Manti, E. Falotico, Y. Mollard, M. Cianchetti, and C. Laschi, "Towards the development of a soft manipulator as an assistive robot for personal care of elderly people," *Int. J. Adv. Robot. Syst.*, vol. 14, no. 2, p. 1729881416687132, 2017.

[8] E. H. Skorina, M. Luo, W. Tao, F. Chen, J. Fu, and C. D. Onal, "Adapting to flexibility: model reference adaptive control of soft bending actuators," *IEEE Robot. Autom. Letters*, vol. 2, no. 2, pp. 964–970, 2017.

[9] J. W. Booth, J. C. Case, E. L. White, D. S. Shah, and R. Kramer-Bottiglio, "An addressable pneumatic regulator for distributed control of soft robots," in *Proc. IEEE Int. Conf. on Soft Robotics*. IEEE, 2018, pp. 25–30.

[10] T. Wang, Y. Zhang, Z. Chen, and S. Zhu, "Parameter identification and model-based nonlinear robust control of fluidic soft bending actuators," *IEEE/ASME Trans. Mechatron.*, vol. 24, no. 3, pp. 1346–1355, 2019.

[11] T. Young, M. Xavier, A. Fleming, and Y. Yong, "A control and drive system for pneumatic soft robots: PneuSoRD." [Online]. Available: https://github.com/PrecisionMechatronicsLab/PneuSoRD

[12] N. El-Atab, R. B. Mishra, F. Al-Modaf, L. Joharji, A. A. Alsharif, H. Alamoudi, M. Diaz, N. Qaiser, and M. M. Hussain, "Soft actuators for soft robotic applications: A review," *Adv. Intell. Syst.*, vol. 2, no. 10, p. 2000128, 2020.

[13] R. Webster III and B. Jones, "Design and kinematic modeling of constant curvature continuum robots: A review," *Int. J. Rob. Res.*, vol. 29, no. 13, pp. 1661–1683, 2010.

[14] J. Wang and A. Chortos, "Control strategies for soft robot systems," *Advanced Intelligent Systems*, vol. 4, no. 5, p. 2100165, 2022.

[15] M. S. Xavier, C. D. Tawk, A. Zolfagharian, J. Pinskier, D. Howard, T. Young, J. Lai, S. M. Harrison, Y. K. Yong, M. Bodaghi, and A. J. Fleming, "Soft pneumatic actuators: A review of design, fabrication, modeling, sensing, control and applications," *IEEE Access*, vol. 10, pp. 59 442–59 485, 2022.

[16] K. Chin, T. Hellebrekers, and C. Majidi, "Machine learning for soft robotic sensing and control," *Adv. Intell. Syst.*, p. 1900171, 2020.

[17] T. George Thuruthel, Y. Ansari, E. Falotico, and C. Laschi, "Control strategies for soft robotic manipulators: A survey," *Soft Robot.*, vol. 5, no. 2, pp. 149–163, 2018.

[18] E. H. Skorina, M. Luo, S. Ozel, F. Chen, W. Tao, and C. D. Onal, "Feedforward augmented sliding mode motion control of antagonistic soft pneumatic actuators," in *Proc. IEEE Int. Conf. on Robotics and Automation*. IEEE, 2015, pp. 2544–2549.

[19] C. Chen, W. Tang, Y. Hu, Y. Lin, and J. Zou, "Fiber-reinforced soft bending actuator control utilizing on/off valves," *IEEE Robot. Autom. Letters*, vol. 5, no. 4, pp. 6732–6739, 2020.

[20] J. van Tiem, J. Groenesteijn, R. Sanders, and G. Krijnen, "3d printed bio-inspired angular acceleration sensor," in *2015 IEEE SENSORS*, 2015-11, pp. 1–4.

[21] A. Marchese, R. Katzschmann, and D. Rus, "A recipe for soft fluidic elastomer robots," *Soft Robot.*, vol. 2, no. 1, pp. 7–25, 2015.

[22] F. Schmitt, O. Piccin, L. Barbé, and B. Bayle, "Soft robots manufacturing: a review," *Front. Robot. AI.*, vol. 5, p. 84, 2018.